Supporting Information:

S1:

There was no instance of Co_3O_4 formation was observed below 473 K, and there was no physical stability of Co_3O_4 thin film was seen beyond 773 K. Hence, the deposition temperature window was chosen between 473 K to 773 K.

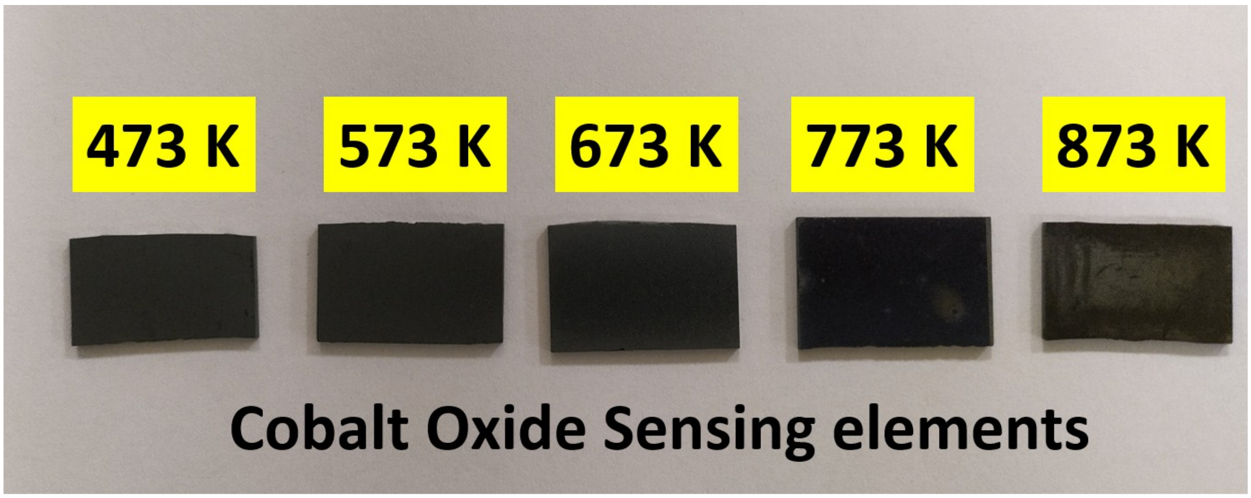

Fig. S1. Photograph of the spray deposited Co_3O_4 thin films at different substrate temperatures.

S2:

To compare the acetone sensing response of the spray deposited Co_3O_4 nanostructure with the commercially purchased cobalt oxide nanoparticles (Co_3O_4, Purity 99%, Alfa-Aesar), the commercially purchased cobalt oxide nanoparticles was drop-casted on to the active area of Ag-Pd electrode as shown in Fig. S2 (d). The sensing characteristics of commercially purchased cobalt oxide nanoparticles and spray deposited Co_3O_4 thin film (deposited at 773 K) are shown in Fig. S1 (a-c). There was no significant acetone sensing response observed for the commercially purchased Co_3O_4 nanoparticles, which indicated that the sensing response not only depends on the sensing material but also dependent on the definite nanostructures, morphology, crystallite size, synthesis/deposition technique, nature of conductivity, phase separation, grains and grain boundary resistances[1–7].

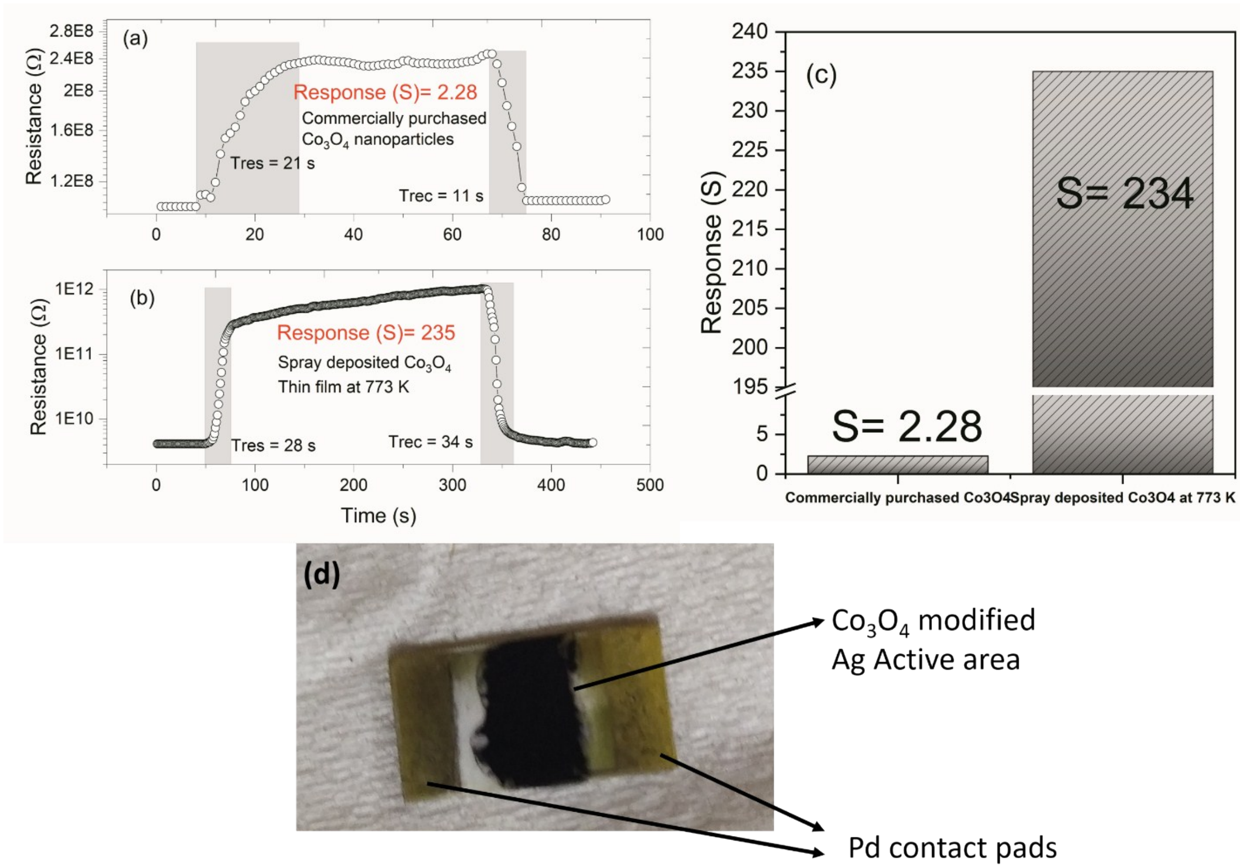

Fig. S2. Acetone transient response of the Co_3O_4 nanostructures (a) commercially purchased nanoparticles, (b) spray deposited Co_3O_4 thin film at 773 K, (c) comparative acetone sensing response of commercially purchased Co_3O_4 nanoparticles and Co_3O_4 thin film at 773 K, and (d) photograph of drop casted Co_3O_4 nanoparticles on active area of Ag-Pd electrode.

S3:

To substantiate this, the structural and morphological analysis of the commercially purchased Co_3O_4 nanoparticles were studied and compared with the spray deposited Co_3O_4 thin film at 773 K, as shown in Fig S2 (a-d). Structural analysis of the commercially available Co_3O_4 nanoparticles revealed the formation of face-centered cubic crystal structure with the preferential plane orientation of 311, whereas the spray deposited Co_3O_4 thin film exhibited the cubic spinel phase with small variations in the lattice parameter. The crystallinity of the commercially purchased Co_3O_4 nanoparticles was observed to be very high in comparison with the spray deposited Co_3O_4 thin film, which would have resulted in the lower sensing response of commercially purchased Co_3O_4 nanoparticles.

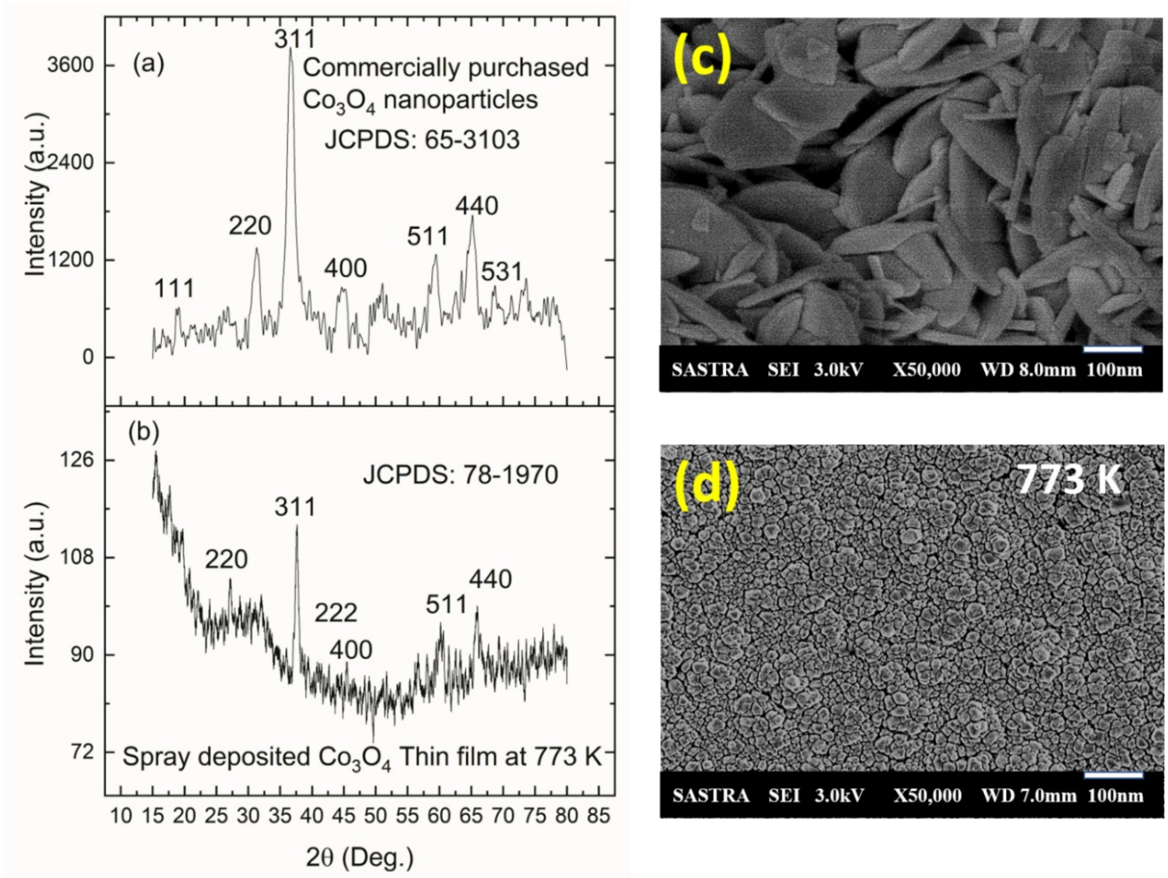

Fig. S3. XRD patterns of the Co_3O_4 nanostructures (a) commercially purchased nanoparticles, (b) spray deposited Co_3O_4 thin film at 773 K and, (c-d) scanning electron micrographs of commercially purchased Co_3O_4 nanoparticles and spray Co_3O_4 thin film at 773 K.

In general, higher the crystallinity of the nanostructures, lower the sensing response [4–7]. In another perspective, the lower sensing response could be attributed to the crystallite size of the nanostructures. Crystal with smaller size possesses enhanced response due to the increased inner grain interaction and transport characteristics during the receptor and transduction function [8]. Smaller nanocrystallites offer increased surface area and surface to volume ratio and improved surface catalytic behavior [5]. The average crystallite size of the commercially purchased Co_3O_4 nanoparticles was found to be 53 nm, whereas spray deposited Co_3O_4 thin films exhibited the crystallite size in the range of 15-35 nm. The larger crystallite size would have resulted in the lower sensing performance of commercially purchased Co_3O_4 nanoparticles[4]. The morphology of the commercial sample exhibited the formation nanoflakes like morphology, whereas spray deposited Co_3O_4 thin film (at 773 K) showed a compact surface with smaller spherical nanograins. This has also reconfirmed the size dependence sensing characteristics of the nanostructures. Thus, the sensing characteristics not only depends on the sensing material but also dependent on the microstructural properties[1–7], morphology[9–15] and synthesis methods [16–19].

References

1 V. E. Bochenkov and G. B. Sergeev, *Adv. Colloid Interface Sci.*, 2005, **116**, 245–254.

2 M. M. Arafat, B. Dinan, S. A. Akbar and A. S. M. A. Haseeb, *Sensors*, 2012, **12**, 7207–7258.

3 R. Boppella, P. Manjula, S. Arunkumar and S. V Manorama, *Chem. Sensors*, 2014, **4**, 1–22.

4 S. Majumdar, *Ceram. Int.*, 2015, **41**, 14350–14358.

5 F. Fang, J. Kennedy, J. Futter, T. Hopf, A. Markwitz, E. Manikandan and G. Henshaw, *Nanotechnology*, 2011, **22**, 335702.

6 P. Srinivasan and J. B. B. Rayappan, *Sensors Actuators B Chem.*, 2018, **277**, 129–143.

7 G. R. Li, T. Hu, G. L. Pan, T. Y. Yan, X. P. Gao and H. Y. Zhu, 2008, 11859–11864.

8 M. J. S. Spencer, *Prog. Mater. Sci.*, 2012, **57**, 437–486.

9 K. S. Kim and Y. J. Park, *Nanoscale Res. Lett.*, 2012, **7**, 47.

10 X. C. Song, X. Wang, Y. F. Zheng, R. Ma and H. Y. Yin, *J. Nanoparticle Res.*, 2011, **13**, 1319–1324.

11 S. G. Victoria, a. M. Ezhil Raj and C. Ravidhas, *Mater. Chem. Phys.*, 2015, **162**, 852–859.

12 W. Shi and N. Chopra, *J. Nanoparticle Res.*, 2011, **13**, 851–868.

13 J. Y. Lao, J. G. Wen and Z. F. Ren, *Nano Lett.*, 2002, **2**, 1287–1291.

14 F. S. Isc and N. D.- Wiirzburg, 2002, 69–89.

15 M. Stan, A. Popa, D. Toloman, T.-D. Silipas and D. C. Vodnar, *Acta Metall. Sin. (English Lett.*, 2016, **29**, 228–236.

16 a Gurlo and M. Ivanovskaya, *Sensors Actuators, B Chem.*, 1997, **44**, 327–333.

17 S. Kannan, L. Rieth and F. Solzbacher, *Sensors Actuators, B Chem.*, 2010, **149**, 8–19.

18 X. D. Gao, X. M. Li and W. D. Yu, *Appl. Surf. Sci.*, 2004, **229**, 275–281.

19 P. V. R. Ramesh, B. K. Ramamurthi and J. V. E. Elangovan, 2015, 4152–4164.